Determination of Transmembrane Protein Structure by Disulfide Cross-Linking: The Escherichia coli Tar Receptor

AA Pakula, and MI Simon

PNAS 1992;89;4144-4148
doi:10.1073/pnas.89.9.4144

Proc. Natl. Acad. Sci. USA
Vol. 89, pp. 4144–4148, May 1992
Biochemistry

Determination of transmembrane protein structure by disulfide cross-linking: The *Escherichia coli* Tar receptor

(chemotaxis/signal transduction/helical bundle)

ANDREW A. PAKULA AND MELVIN I. SIMON

Division of Biology, California Institute of Technology, Pasadena, CA 91125

Contributed by Melvin I. Simon, January 30, 1992

ABSTRACT **We have devised a generally applicable strategy for analysis of protein structure and have applied it to examine the structure of the transmembrane portion of the Tar receptor of *Escherichia coli*. The basis of our approach is the use of disulfide cross-linking to identify residues that are within close proximity. To generate and test large numbers of cysteine pairs, we used an unusual method of mutagenesis by which cysteine substitutions can be created randomly at a number of targeted codons. Cysteine-substituted proteins encoded by mutagenized genes may be screened directly for disulfide formation within oligomers or, alternatively, different pools of genes may be randomly recombined to generate gene populations with substitutions in multiple regions. Thus, it is possible to detect a variety of disulfide cross-links between and within individual protein molecules. Interactions between the four membrane-spanning stretches of the Tar dimer were probed by measuring the tendency of 48 cysteine substitutions throughout this region to form disulfide cross-links with one another. We have interpreted these data to suggest a helical-bundle structure for the transmembrane region. The four helices of this bundle are not structurally equivalent: the two TM1 helices interact closely, whereas the TM2 helices are more peripherally located.**

The Tar receptor of *Escherichia coli* is a transmembrane signal transducer protein involved in the detection of chemotactic effectors. It is a member of a family of related receptors, the methyl-accepting chemotaxis proteins, which share considerable amino acid sequence similarity (1). Tar appears to act as a dimer (2). It mediates repellent responses to nickel and cobalt ions and attractant responses to aspartate and maltose (3). Each 553-amino acid monomer of Tar is comprised of relatively large periplasmic and intracellular domains as well as two membrane-spanning domains that are thought to be α-helical (4). (The transmembrane topology of Tar is illustrated in Fig. 1.) Ligands bind to the periplasmic region of Tar (5–8) leading the receptor to modulate the activity of the soluble autophosphorylating kinase CheA (9, 10). This initial event leads, through a series of additional intracellular interactions, to altered bacterial swimming behavior.

The nature of the protein conformational changes that mediate communication across lipid bilayers is unknown. The Tar receptor resembles the mammalian epidermal growth factor and insulin receptors in that each of these proteins consists of large soluble domains linked by a small number of transmembrane stretches. In contrast to the epidermal growth factor receptor, the oligomeric state of the Tar receptor does not change as a consequence of ligand binding (2); thus any structural changes involved in transmembrane signal transmission occur within the preformed receptor dimer. We presume that ligand binding results in a conformational change in the periplasmic domain and that this change is then propagated by the four transmembrane domains to the cytoplasmic domain. The structure of the isolated periplasmic domain of the Tar protein of *Salmonella typhimurium* was recently solved by x-ray crystallography (11). Analysis of this structure indicates that ligand binding induces a shift in the relative orientation of the receptor monomers. An understanding of the nature of the transmembrane conformational changes will require three-dimensional structural information for the membrane-spanning domains—a goal that has been frustrated by difficulties encountered in preparing crystals of intact methyl-accepting chemotaxis proteins. Accordingly, our current efforts have focused on development of a structural model of the Tar transmembrane domains through biochemical means.

We have used a cysteine disulfide cross-linking approach to analyze the structure of the Tar transmembrane domains. Disulfide cross-linking using small numbers of naturally occurring or engineered cysteine residues has been employed to probe protein structure (2, 12–19). We have now introduced methods that make it possible to analyze protein structure in detail by this approach. Through the use of an unusual procedure for oligonucleotide synthesis, individual cysteine substitutions were introduced at nearly every position in the transmembrane region. We then determined which cysteines are sufficiently close to form disulfide cross-links. The resulting information places strong constraints upon the possible arrangements of the transmembrane helices, and thus we have been able to propose a structure for this region. This strategy is generally applicable but is particularly well suited for analysis of transmembrane domain structure since the secondary structure of such regions is often known and since structural information is nearly inaccessible by other means.

MATERIALS AND METHODS

Bacterial Strains and Plasmids. In all experiments, Tar is expressed from plasmid pAP200, which was constructed by the addition of the M13 origin of replication from plasmid pZ150 (20) to pRBB5 (R. Bourret, personal communication). pRBB5 was derived from pAK101 (5) by engineering restriction sites *Spe* I, *Avr* II, *Pst* I, *Bsp*M2, and *Xho* I within the TM1 coding region while preserving the wild-type amino acid sequence (Fig. 2). *E. coli* KO607 (21) and HCB721 (22) lack functional methyl-accepting chemotaxis proteins genes. Additionally, HCB721 lacks functional *cheR* and *cheB* genes.

Introduction of Cysteine Substitutions. Double-stranded oligonucleotide cassettes for TM1 mutagenesis were ligated to pAP200 DNA (Fig. 2). Mutagenesis of TM2 was performed by site-directed mutagenesis (23) of M13AP1 single-stranded DNA. M13AP1 is an M13mp19 (24) containing the *Xba* I–*Kpn* I restriction fragment of pAP200. Replicative-form DNA from pooled mutagenized M13AP1 candidates was digested with *Xba* I and *Kpn* I restriction enzymes, and the TM2-

The publication costs of this article were defrayed in part by page charge payment. This article must therefore be hereby marked "*advertisement*" in accordance with 18 U.S.C. §1734 solely to indicate this fact.

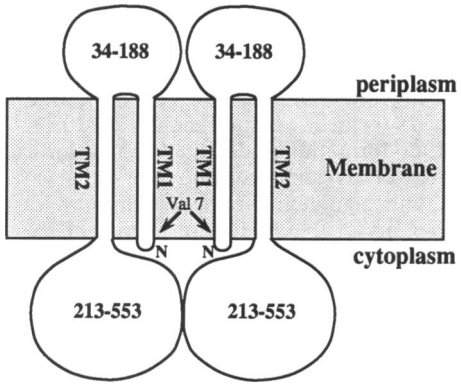

FIG. 1. Transmembrane topology of Tar. Each Tar monomer consists of 553 amino acids. The periplasmic and cytoplasmic domains are directly linked by TM2, a transmembrane region of 24 amino acids. TM1 is located close to the amino terminus of Tar and is 27 amino acids long.

containing fragment was religated to pAP200. Mutagenized DNA was used to transform strain KO607. Nonchemotactic isolates were identified as probable *tar* deletion mutants and excluded from further analysis.

Cysteine Mutant Recombination. Pools of plasmids bearing *tar* genes with cysteine substitutions in both transmembrane regions were prepared by random recombination *in vitro* of *Eco*RI–*Xba* I DNA fragments bearing substituted TM1 and TM2 regions. Two separate pools were prepared. For pool A, genes with cysteine mutations at TM1 residues 7–25 and TM2 residues 201–212 were recombined. Cysteine substitutions of TM1 residues 15–33 and TM2 residues 189–200 were recombined for pool B. Recombinant plasmid DNA was introduced into strain HCB721, and individual transformants were selected for cross-linking analysis as described below. [Cys^{25},Cys^{189}] and [Cys^{25},Cys^{192}]Tar variants were individually constructed in a similar manner.

Mutagenic Oligonucleotide Synthesis. Mutagenic oligonucleotides were synthesized by a variation of a protocol developed by M. Zollar and D. Botstein (personal communication). Two solid-phase DNA synthesis columns were operated simultaneously, and resin support with partially completed oligonucleotides was periodically exchanged between the two columns. One column was programmed to synthesize the wild-type sequence, and the other was programmed for the repeated synthesis of a cysteine codon. To achieve 10% substitutions per codon, the first targeted codon was synthesized with 10% of the resin in the cysteine column and the remainder in the wild-type sequence column. After the synthesis of each codon, all resin was removed, mixed, and redistributed as before.

Disulfide Cross-Linking Analysis. Saturated cultures (150 μl) of HCB721 or KO607 carrying mutant candidate pAP200 plasmids in LB broth with ampicillin (100 μg/ml) were centrifuged at 600 × *g* for 15 min. Cell pellets were resuspended in 50 μl of TG [50 mM Tris·HCl, pH 7.5/10% (vol/vol) glycerol] containing 1 mM $MgCl_2$, DNase I (10 μg/ml), RNase A (10 μg/ml), and lysozyme (0.5 mg/ml), incubated on ice for 20 min, and lysed by five freeze/thaw cycles. The lysate was mixed with 50 μl of 1.0 mM aqueous iodine, incubated for 15 min at 20°C, and centrifuged again. The pellet was resuspended in 20 μl of TG, mixed with 15 μl of sample buffer [0.32 M Tris·HCl, pH 6.8/8% (wt/vol) SDS/40% glycerol/0.01% bromphenol blue] including 0.2 M sodium iodoacetate. Samples (15 μl) were heated to 90°C for 3 min and subjected to electrophoresis in SDS/7% polyacrylamide gels (25). Tar was detected by Western blot analysis (26) using specific antibodies, an enzyme-linked secondary antibody, and appropriate detection reagents (Promega Protoblot or Amersham ECL system). DNA sequencing was performed using double-stranded pAP200 template DNA and the Sequenase system (United States Biochemical).

Computer Modeling. Molecular dynamics and energy minimization calculations were performed using BIOGRAF (BioDesign, New York) run on the DEC VAXstation 3500 computer. For disulfide-forming residue pairs, the distance between β-carbons was constrained to 4.2 Å.

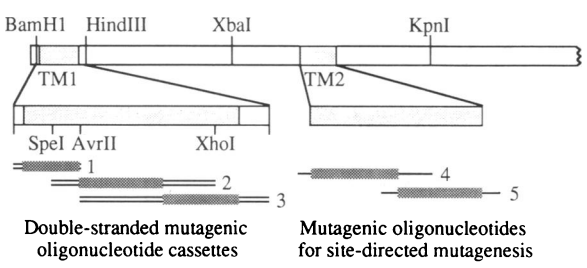

FIG. 2. Introduction of cysteine substitution mutations in the *tar* gene of pAP200. Shaded regions of single- or double-stranded oligonucleotides indicate regions into which cysteine substitutions were randomly introduced.

RESULTS

Random Introduction of Cysteine Substitution Mutations. Potential TM1 cysteine mutants generated using cassettes 1 and 2 (Fig. 2) were sequenced directly without prior screening for disulfide formation or receptor function. A large fraction of these isolates (30%) sustained small deletion mutations. Subsequently, deletion mutants were identified by prescreening candidates for chemotactic function. Whereas each of the cysteine substitution mutants retained substantial activity, deletion mutations resulted in a nonchemotactic phenotype. The average number of cysteine substitutions generated per isolate was close to the expected number in most experiments (data not shown). Furthermore, cysteine substitutions appeared to be distributed randomly among the targeted residues (Fig. 3).

Homologous Disulfide Cross-Linking. We initially assembled a set of plasmid-borne mutant *tar* genes containing cysteine substitutions at nearly all TM1 and TM2 residue positions (Table 1). These substitutions were introduced by using synthetic oligonucleotides. Upon oxidation, pairs of homologous cysteine residues (i.e., the corresponding residues of the two monomers of the Tar dimer) may form intermolecular disulfide bridges. After oxidation with iodine, disulfide cross-linked forms of Tar were identified by their

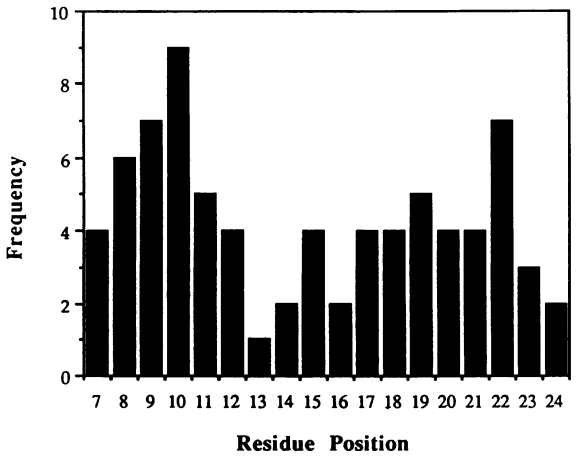

FIG. 3. Distribution of cysteine substitutions generated with mutagenic cassettes 1 and 2 (see Fig. 2) among targeted positions.

Table 1. Cysteine substitution mutants and their homologous cross-linking efficiencies

Cysteine(s) in TM1, position(s)	TM1–TM1 cross-linking	Cysteine(s) in TM2, position(s)	TM2–TM2 cross-linking
7	+	189	−
8	−	190	−
9	−	191	−
10	−	192	−
11	++	193	−
10, 12	−	195	−
13	−	196	−
14	+	189, 192, 197	+
15	+	198	−
15, 16	+	200	−
17, 20	+	201, 203	+
18	+	202, 204	−
19	+	203	−
20	−	204	+
21	+	204, 205	+
22	++	206	−
23	−	203, 207, 210	−
24	−	207	−
25	++	208	+
26	−	209	−
27	−	211	+
28	−	210, 212	−
29	++		
30	−		
31	−		
32	−		
33	+		

+, Detectable cross-linking at 5 to 20% efficiency; ++, >50% efficiency; −, no detectable cross-linking (<5%).

distinct electrophoretic mobilities (Fig. 4). Since there are no cysteines in wild-type Tar, any observed Tar cross-linking is due to the experimentally introduced substitutions. For isolates bearing multiple substitutions, the cysteine residues participating in disulfide formation were identified by comparison with mutant *tar* genes that contained only one or the other substitution. To determine whether reaction of iodine with other Tar amino acid side chains might alter the native structure of Tar, we examined the effect of iodine treatment on the ability of wild-type Tar to stimulate CheA autophosphorylation *in vitro* (9, 10). Substantial Tar activity was retained (L. Alex and A.A.P., unpublished data); thus, it is unlikely that iodine treatment significantly perturbs Tar structure.

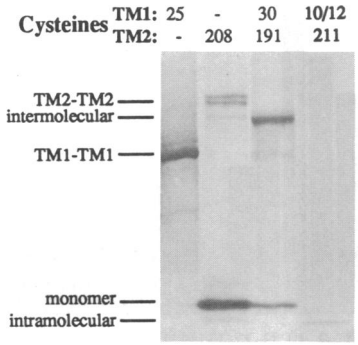

FIG. 4. SDS/gel electrophoretograms of representative cysteine-substituted Tar proteins after iodine oxidation. The electrophoretic mobility of monomeric Tar and of each cross-linked form is indicated. Proteins were visualized immunologically.

Of the 48 "homologous" cysteine pairs tested, only four were found to form disulfide bonds efficiently (with >50% yield); these involved positions 11, 22, 25, and 29 of TM1 (Table 1). An additional nine TM1–TM1 and five TM2–TM2 disulfide pairs formed, but inefficiently (5–20%). Thus, efficient disulfide formation under these conditions identifies a small subset of cysteine residue pairs that are in close proximity. This high degree of specificity may result in part from the rapidity of the oxidation reaction. Cross-linking is completed within 15 sec of iodine addition (data not shown).

When TM1 and TM2 are modeled as α-helices, the homologous disulfide-forming positions are found only on one side of each helix (Fig. 5). This observation supports the supposition that TM1 and TM2 are essentially α-helical. Furthermore, the asymmetric distribution of these positions suggests the gross orientation of the four transmembrane helices of the Tar dimer. We expect that the helical face upon which disulfide-forming residues are found is directed toward its homologue in the other monomer.

Heterologous Disulfide Cross-Linking. The homologous disulfide bonds described above probe two (TM1–TM1 and TM2–TM2) of the four sets of pairwise transmembrane domain interactions that could occur in the three-dimensional structure of Tar. To probe TM1–TM2 interactions either within (intramolecular) or between monomers (intermolecular) of the Tar dimer, we examined Tar variants with cysteine substitutions in both transmembrane domains. Plasmids expressing such variants were prepared by random recombination of pools of TM1 and TM2 cysteine mutants. Candidates from the recombinant plasmid pools were then screened for disulfide formation.

Of 192 isolates examined, 15 expressed variant Tar proteins that formed disulfide cross-links efficiently. The *tar* genes of these isolates were then analyzed by DNA sequencing to determine the sites of the relevant cysteine residues. Both intermolecular and intramolecular disulfides between TM1 and TM2 were identified (Table 2). Thus, each TM1 helix appears to interact with both of the TM2 helices in the Tar dimer.

Structural Modeling. We have used computer-aided molecular modeling to construct a structural model for the Tar transmembrane structure based on cross-linking data. For this purpose, we considered only the heterologous and ho-

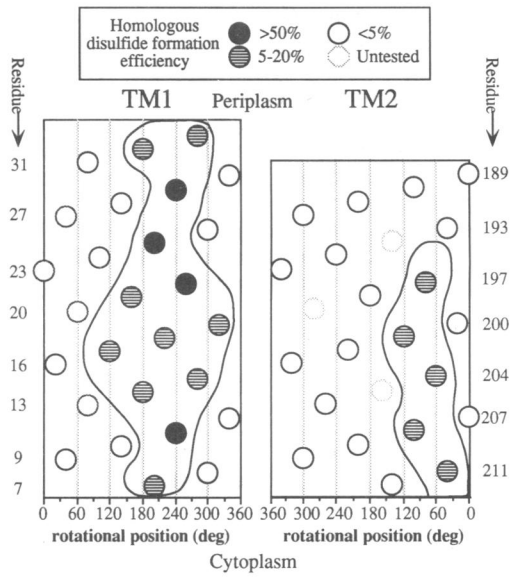

FIG. 5. Homologous disulfide formation by cysteines in TM1 and TM2. The transmembrane α-helices are shown in a two-dimensional representation and each residue is indicated by a circle. deg, Degree(s).

Table 2. Tar residue positions of cysteine substitutions that result in efficient (>50%) TM1–TM2 disulfide formation

Intermolecular disulfide bond, position(s)		Intramolecular disulfide bond, position(s)	
TM1	TM2	TM1	TM2
10/12	208	7	211
10/12	209	10	211
11	210/212	10/12	211
15	208	11	211
19	208	15	204
30	191	21	201/203
30	193	25	189/192/197*
33	189	28	193

*This cross-link appears to involve Cys^{25} and Cys^{197} because for [Cys^{25},Cys^{189}]- and [Cys^{25},Cys^{192}]Tar variants heterologous cross-links do not form.

mologous cross-links that form efficiently. Inefficient cross-linking positions are presumably separated by greater distances and were not considered for detailed model building. We also excluded from consideration those isolates for which, because of the number of cysteine substitutions, the residues that participate in disulfide formation could not be identified unambiguously.

Four α-helices of appropriate length were constructed and arranged parallel to one another with their termini oriented as dictated by the known transmembrane topology of Tar. The helices were then rotated on their long axes so that residue pairs that form cross-links were roughly oriented toward one another. To reduce computational complexity, methyl groups were substituted for each amino acid side chain. Molecular dynamics simulation and energy minimization calculations were performed using distance and angle constraints between β-carbons at disulfide-forming residue positions. The structures were also constrained to remain α-helical. The distance between β-carbons in the final model is 4.6 ± 0.7 Å (mean ± SD). The resulting structure is essentially an α-helical bundle; however, the four helices are not structurally equivalent (Fig. 6). The TM1 helices are located centrally and interact extensively with one another. The central position of the TM1 helices is not dependent on the initial orientation of the helices; a similar structure results if TM2 helices are placed in close proximity at the start of molecular modeling calculations.

DISCUSSION

We have developed and demonstrated a generally applicable strategy for analysis of protein structure; this strategy involves the introduction and cross-linking analysis of large numbers of cysteine residue pairs. The feasibility of this approach depends strongly on a technique for the random introduction of cysteine substitutions. A pool of single or multiple cysteine substitution mutants may thus be assembled, and the encoded protein variants may be screened for disulfide formation directly without prior determination of DNA sequence changes. It is also possible to identify positions between which disulfide formation does not occur. Since cysteine substitutions are randomly distributed among the targeted positions, the probability that any particular cysteine substitution or pair of cysteine positions is present in the mutant pool can be readily calculated.

The interpretation of limited disulfide cross-linking data in terms of three-dimensional structure is complicated by the fact that interatomic distances cannot be determined directly from the rate or efficiency of disulfide formation. By examining the cross-linking behavior of a large fraction of all possible cysteine pairs within a given structural element, this

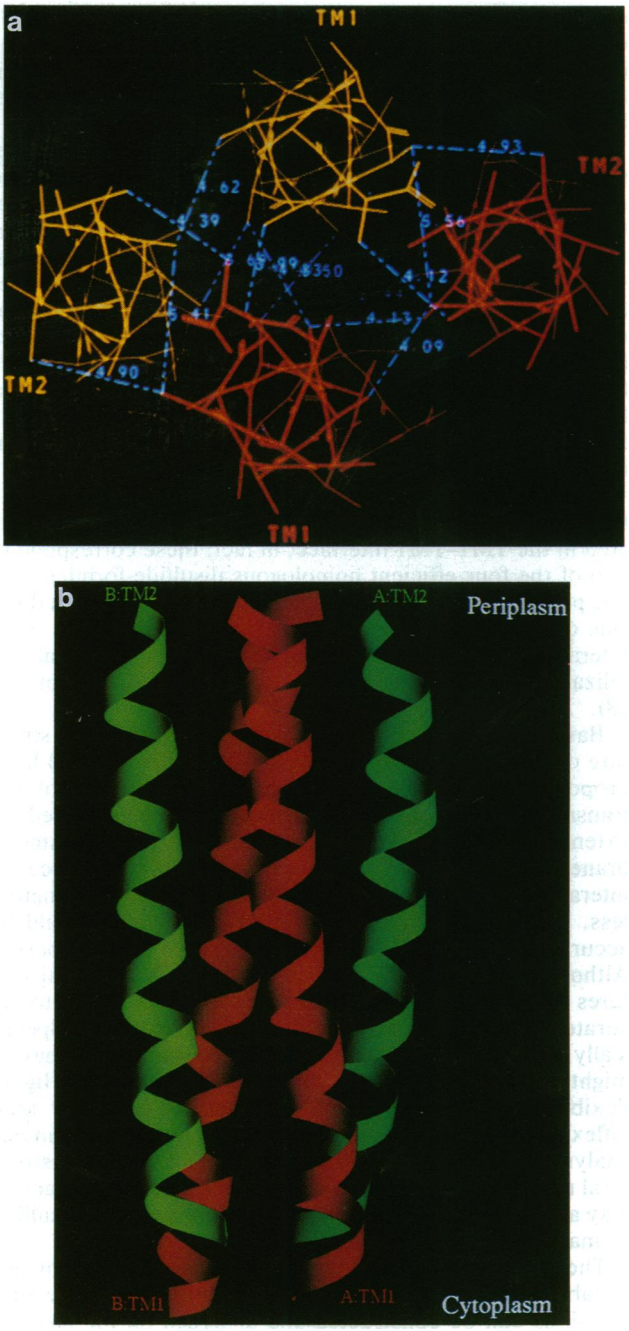

FIG. 6. Structural model for the Tar transmembrane domains. (*a*) Helical-bundle structure as viewed end on from the periplasm. Helices that belong to the same Tar monomer are shown in the same color. Distances between β-carbons that were constrained during molecular modeling are shown in blue. (*b*) Ribbon diagram of the structural model. TM1 helices are shown in red; TM2 are in green. Letters "A" and "B" indicate which helices are located within the same Tar monomer.

obstacle may be overcome. Cysteine pairs that cross-link most and least readily may be assumed to be closest and farthest apart, respectively, and model building can be performed on this basis. Furthermore, because model building considers a large number of interactions with equal weight, the effects of unusual or misleading results on the final structure will be minimal.

Extensive amino acid sequence similarities exist between Tar and other related receptors in the region of TM1 and less so in TM2 (1). If wild-type side chains are modeled into the proposed helical-bundle structure, all but one of the 14 highly

conserved transmembrane residues are found to be capable of participating in at least one interhelical interaction. The conservation of these amino acids presumably reflects their important structural and/or functional roles; thus this correlation provides support for our model.

The inefficiently forming homologous cysteine pairs described above generally fall in the interior of the predicted α-helical bundle structure. We presume that disulfide formation between these distant positions occurs as the receptor, undergoing random structural fluctuations, momentarily assumes a variety of alternative conformations. In some cases these fluctuations must involve rather large-scale molecular motions, on the order of 10 Å. Nonetheless, they do not seem to involve complete loss of folded structure since disulfide formation is not observed between residues located on exterior helical faces. A high degree of flexibility for the soluble domains of Tar has been suggested (14) on the basis of measurements of cysteine cross-linking rates.

Of the three highly conserved hydrophilic residues in the transmembrane domains, two (Gln-22 and Ser-25) are situated in the TM1–TM1 interface; in fact, these correspond to two of the four efficient homologous disulfide-forming residue positions. Hydrogen-bonding interactions between these side chains might stabilize the TM1–TM1 interaction. Such interactions could contribute significantly to structural stabilization as a result of their hydrophobic environment (27, 28).

Based on the recently determined three-dimensional structure of the Tar periplasmic domain, Milburn *et al.* (11) have proposed a model for the structural arrangement of the transmembrane domains. This model was constructed by extension of long periplasmic α-helices into the transmembrane region and thus is not based upon direct evidence for interactions between the transmembrane helices. Nonetheless, the overall topology predicted in this way should be accurate and is identical to the topology we have proposed. Although our approach may correctly predict general features of transmembrane domain structure; its ability to accurately characterize structural details is uncertain. Specifically, cysteine pairs with similar cross-linking behavior might actually be separated by different distances. Highly flexible helical regions might interact more readily than inflexible ones and thus appear inappropriately close in our analysis. Differential accessibility by iodine to various structural regions might produce similar effects and steric factors may also play a role in determining the efficiency of disulfide formation.

The structural model that we have described provides testable predictions. For example, additional cysteine substitutions can be constructed and analyzed on the basis of residue proximity in the model. Furthermore, residues that appear to be intimately involved in helical interactions are logical targets for directed mutagenesis. We expect that disruption of such interactions will result in informative signaling phenotypes. Finally, we anticipate that the use of similar cross-linking techniques will help to reveal the transmembrane conformational changes that play a role in signal transduction.

We thank David Botstein for communication of unpublished methods for oligonucleotide synthesis; James Bowie and Yun Sun for suggestions on molecular modeling calculations; AnnaMarie Aquinaldo, Conrad Sevilla III, and Brett Znider for oligonucleotide synthesis; Robert Bourret, Doug Rees, and Andy Myers for helpful comments and discussion. This work was supported by National Institutes of Health Grant AI 19296 and by a grant from the Markey Foundation. A.A.P. is the recipient of a postdoctoral fellowship from the American Cancer Society, California division.

1. Dahl, M. K., Boos, W. & Manson, M. D. (1989) *J. Bacteriol.* **171,** 2361–2371.
2. Milligan, D. L. & Koshland, D. E., Jr. (1988) *J. Biol. Chem.* **263,** 6268–6275.
3. Springer, M. S., Goy, M. F. & Adler, J. (1977) *Proc. Natl. Acad. Sci. USA* **74,** 3312–3316.
4. Manoil, C. & Beckwith, J. (1986) *Science* **233,** 1403–1408.
5. Krikos, A., Conley, M. P., Boyd, A., Berg, H. C. & Simon, M. I. (1985) *Proc. Natl. Acad. Sci. USA* **82,** 1326–1330.
6. Russo, A. F. & Koshland, D. E., Jr. (1983) *Science* **220,** 1016–1020.
7. Boyd, A., Kendall, K. & Simon, M. I. (1983) *Nature (London)* **301,** 623–626.
8. Krikos, A., Mutoh, N., Boyd, A. & Simon, M. I. (1983) *Cell* **33,** 615–622.
9. Borkovich, K. & Simon, M. (1990) *Cell* **63,** 1339–1348.
10. Borkovich, K. A., Kaplan, N., Hess, J. F. & Simon, M. I. (1989) *Proc. Natl. Acad. Sci. USA* **86,** 1208–1212.
11. Milburn, M., Privé, G., Milligan, D., Scott, W., Yeh, J., Jancarik, J., Koshland, D., Jr., & Kim, S.-H. (1991) *Science* **254,** 1342–1347.
12. Karlin, A., Holtzman, E., Yodh, N., Lobel, P., Wall, J. & Hainfeld, J. (1983) *J. Biol. Chem.* **258,** 6678–6681.
13. Bubis, J. & Khorana, H. G. (1990) *J. Biol. Chem.* **265,** 12995–12999.
14. Falke, J. J. & Koshland, D. E., Jr. (1987) *Science* **237,** 1596–1600.
15. Falke, J. J., Dernburg, A. F., Sternberg, D. A., Zalkin, N., Milligan, D. L. & Koshland, D. E., Jr. (1988) *J. Biol. Chem.* **263,** 14850–14858.
16. Karnik, S. S. & Khorana, H. G. (1990) *J. Biol. Chem.* **265,** 17520–17524.
17. First, E. A. & Taylor, S. S. (1984) *J. Biol. Chem.* **259,** 4011–4014.
18. Kurtenbach, E., Curtis, C. A., Pedder, E. K., Aitken, A., Harris, A. C. & Hulme, E. C. (1990) *J. Biol. Chem.* **265,** 13702–13708.
19. Lynch, B. & Koshland, D., Jr. (1991) *Proc. Natl. Acad. Sci. USA* **88,** 10402–10406.
20. Zagursky, R. J. & Berman, M. L. (1984) *Gene* **27,** 183–191.
21. Oosawa, K., Mutoh, N. & Simon, M. I. (1988) *J. Bacteriol.* **170,** 2521–2526.
22. Wolfe, A. J., Conley, M. P. & Berg, H. C. (1988) *Proc. Natl. Acad. Sci. USA* **85,** 6711–6715.
23. Kunkel, T. (1985) *Proc. Natl. Acad. Sci. USA* **82,** 488–492.
24. Yanisch-Perron, C., Vieira, J. & Messing, J. (1985) *Gene* **33,** 103–119.
25. Laemmli, U. (1970) *Nature (London)* **227,** 680–685.
26. Tsang, V., Peralta, J. & Simons, A. (1983) *Methods Enzymol.* **92,** 377–391.
27. Klotz, I. M. & Franzen, J. S. (1962) *J. Am. Chem. Soc.* **84,** 3461–3466.
28. Singer, S. J. (1990) *Annu. Rev. Cell Biol.* **6,** 247–296.